Iterative schemes for surfactant transport in porous media

D. Illiano, I.S. Pop, F.A. Radu

UHasselt Computational Mathematics Preprint
Nr. UP-19-05

May 31, 2019

Noname manuscript No.
(will be inserted by the editor)

Iterative schemes for surfactant transport in porous media

Davide Illiano · Iuliu Sorin Pop · Florin Adrian Radu

Received: date / Accepted: date

Abstract In this work we consider the transport of a surfactant in a variably saturated porous media. The water flow is modelled by the Richards equations and it is fully coupled with the transport equation for the surfactant. Three linearization techniques are discussed: the Newton method, the modified Picard and the L-scheme. Based on these, monolithic and splitting schemes are proposed and their convergence is analyzed. The performance of these schemes is illustrated on four numerical examples. For these examples, the number of iterations and the condition numbers of the linear systems emerging in each iteration are presented.

Keywords Richards equation · reactive transport · linearization schemes · L-scheme · modified Picard · Newton method · splitting solvers

1 Introduction

Many societally relevant problems are involving multiphase flow and multicomponent, reactive transport in porous media. Examples in this sense appear in the enhanced oil recovery, geological CO_2 storage, diffusion of medical agents into the human body, or water or soil pollution. In all these situations, experimental results are difficult to obtain, if not possible at all, and therefore numerical simulations become a key technology. The mathematical models for problems as mentioned above are (fully or partially) coupled, non-linear, possible degenerate partial differential equations. In most cases, finding explicit solutions is not possible, whereas developing appropriate

Project founded by VISTA, a collaboration between the Norwegian Academy of Science and Letters and Equinor.

Davide Illiano, Florin Adrian Radu
Department of Mathematics, University of Bergen, Allegaten 41, Bergen, Norway
E-mail: {Davide.Illiano, Florin.Radu}@uib.no

Iuliu Sorin Pop
Faculty of Sciences, University of Hasselt, Agoralaan Building D, BE 3590 Diepenbeek, Belgium
E-mail: sorin.pop@uhasselt.be

algorithms for finding numerical solutions is a challenge in itself. Here we investigate robust and efficient methods for solving the nonlinear problems obtained after performing an implicit time discretization, the focus being on iterative, splitting or monolithic schemes for fully coupled flow and transport.

Of particular interest here is the special case of multiphase, reactive flow in porous media, namely the surfactant transport in soil [2,20,32,23,26,27]. Surfactants, which are usually organic compounds, are commonly used for actively combating soil and water pollution [17,37,12,42,13]. They contain both hydrophobic and hydrophilic groups and are dissolved in the water phase, being transported by diffusion and convection. Typically, the surfactants are employed in soil regions near the surface (vadose zone), where water and air are present in the pores. Consequently, the outcoming mathematical model accounts the transport of at least one species (the surfactant, but often also the contaminant) in a variably saturated porous medium. Whereas the dependence of the species transport on the flow is obvious, one can encounter the reverse dependece as well since if the surfactants are affecting the interfacial tension between water and air, leading to a dependency of the water flow on the concentration of surfactant. In other words, one has to cope with a fully coupled flow and transport problem, and not only with a one-way coupling, i.e. when only the transport depends on the flow, as mostly considered in reactive transport [34].

Whereas the surfactant transport is described by a reaction-diffusion-convection equation, water flow in variably saturated porous media is modelled by the Richards equation [7,19]. The main assumption in this case is that the air remains in contact with the atmosphere, having a constant pressure (the atmospheric pressure, here assumed zero). This allows reducing the flow model to one equation, the Richards' equation. In mathematical terms, this equation is degenerate parabolic, whose solution has typically low regularity [3].

From the above, and adopting the pressure head as the main unknown in the Richards' equation, we study here different linearization schemes for the model

$$\frac{\partial \theta(\Psi,c)}{\partial t} - \nabla \cdot (K(\theta(\Psi,c))\nabla(\Psi+z)) \;=\; H_1 \tag{1}$$

and

$$\frac{\partial \theta(\Psi,c)c}{\partial_t} - \nabla \cdot (D\nabla c - \mathbf{u_w}c) + R(c) \;=\; H_2, \tag{2}$$

holding for $\mathbf{x} \in \Omega$ (z being the vertical coordinate of $\mathbf{x}$, pointing against gravity) and $t \in (0,T]$. Here Ω is a bounded, open domain in $\mathbb{R}^d$ ($d = 1,2$ or 3) having a Lipschitz continuous boundary $\partial\Omega$ and $T > 0$ is the final time. Further, $\theta(\cdot,\cdot)$ denotes the water content, and is a given function depending on the pressure head Ψ and of the surfactant concentration c. Also, $K(\cdot)$ is the hydraulic conductivity, $D > 0$ the diffusion/dispersion coefficient. Finally, $\mathbf{u_w}$ is the water flux, $R(\cdot)$ the reaction term expressed as a function of the concentration c, and H_1, H_2 are the external sinks/sources. Initial and boundary conditions, which are specified below, complete the system.

We point out that the water content and the hydraulic conductivity, $\theta(\cdot,\cdot)$ and $K(\cdot)$ are given non-linear functions. They are medium- and surfactant-dependent and are determined experimentally (see [19]). Specific choices are provided in Section 2.

To solve numerically the system (1) – (2) one needs to discretize it in time and space. We refer to [16] for a practical review of numerical methods for the Richards equation. Due to the low regularity of the solution and the need of relatively large time steps, the backward Euler method is a good candidate for the time discretization. Multiple spatial discretization techniques are available, such as the Galerkin Finite Element Method (*FEM*) [31,5,38], the Mixed Finite Element Method (*MFEM*) [4, 25,35,43,44], the Multi-Point Flux Approximation (*MPFA*) [24,6,1] and the Finite Volume Method (*FVM*) [10,14,15].

Since the time discretization is not explicit, the outcome is a sequence of nonlinear problems, for which a linearization step has to be performed. Widely used linearization schemes are the quadratic, locally convergent Newton method and the modified Picard method [11]. For both, the convergence is guaranteed if the starting point is close to the solution. For evolution equations, as the initial guess is typically the solution at the previous time, this still induces severe restrictions on the time step (see [36]). This aspect is improved in [9] by a switch of variable and through a stabilized approach in [22]. Alternative approaches are the L-scheme (see [45,39, 33,29] and the modified L-scheme [30], both being robust w.r.t. the mesh size, but converging linearly. In particular, the L-scheme converges for any starting point, and the restriction on the time step, if any, is very mild. The modified L-scheme makes explicit use of the choice of the starting point as the solution obtained at the previous time, and has an improved convergence behavior if the changes in the solutions at two successive times are controlled by the time step. Moreover, the robustness of the Newton method is significantly increased if one considers combinations of the Picard and the Newton methods [8], and in particular of the L-scheme and the Newton scheme [29].

We conclude this discussion by mentioning that in this paper we adopt the *FEM* and the *MPFA*, but the iterative schemes presented here can be applied in combination with any other spatial discretization method. The focus is on effectively solving the fully coupled flow and transport system (1) – (2), and in particular on the adequate treating of the coupling between the two model components (the flow and the reactive transport). The schemes are divided in three main categories: monolithic (MON), non-linear splitting (NonLinS) and alternate splitting (AltS). Subsequently, we denote e.g. by MON-NE, the monolithic scheme obtained by applying the Newton method as linearization. The nonlinear splitting schemes (NonLinS) should be understood as solving at each time step first the flow equation until convergence, by using the surfactant concentration from the last iteration, and then with the obtained flow solving the transport equation until convergence. The procedure can be continued iteratively, this being the usual *or classical* splitting method for transport problems. The convergence of NonLinS does not depend on the linearization approach used for each model component (Newton, Picard or $L-$scheme), because we assume that the nonlinear subproblems are solved exactly, i.e. until convergence. Finally, the alternate splitting methods (AltS) have a different philosophy. Instead solving each subproblem until convergence within each iteration, one performs only one step of the chosen linearization. For example, AltS-NE will perform one Newton step for each moel component, and iterate. These schemes are illustrated in Figures 1, 2.

All the schemes can be analysed theoretically, and we do this exemplary for MON-LS, i.e. for the monolithic approach combined with the L-scheme. Based on comparative numerical tests performed for academic and benchmark problems, we see that the alternate methods can save substantial computational time, while maintaining the robustness of the L-scheme.

The remaining of the paper is organized as follows. In Section 2 we establish the mathematical model and the notation used and present the iterative monolithic and splitting schemes. In Section 3 we prove the convergence of the $MON-LS$ scheme and briefly discuss the convergence of the other schemes. Section 4 presents four different numerical examples. They are inspired by the cases already studied in the literature [29,26]. Section 5 concludes this work.

2 Problem formulation, discretization and iterative schemes

We solve the fully coupled system (1)–(2), completed by homogeneous Dirichlet boundary conditions for both Ψ and c and the initial conditions:

$$\Psi = \Psi_0 \text{ and } c = c_0 \text{ at } t = 0.$$

We use the van Genuchten-Mualem parameterization [18]

$$\theta(\Psi) = \begin{cases} \theta_r + (\theta_s - \theta_r)\left(\frac{1}{1+(-\alpha\Psi)^n}\right)^{\frac{n-1}{n}}, & \Psi \leq 0 \\ \theta_s, & \Psi > 0, \end{cases} \tag{3}$$

$$K(\theta(\Psi)) = \begin{cases} K_s\theta(\Psi)^{\frac{1}{2}}\left[1-\left(1-\theta(\Psi)^{\frac{n}{n-1}}\right)^{\frac{n-1}{n}}\right], & \Psi \leq 0 \\ K_s, & \Psi > 0, \end{cases} \tag{4}$$

where θ_r and θ_s represent the values of the residual and saturated water content, K_s is the conductivity and α and n are model parameters depending on the soil.

Observe that in the expression above for θ the influence of the surfactant on the water flow is neglected. As reported in [21,26,41], the surface tension between water and air does depend on the surfactant concentration c, implying the same for the function θ above. The following parametrization is proposed in [26]

$$\theta(\Psi, c) := \theta\Big(\frac{\gamma(c)}{\gamma_0(c_0)}\Psi\Big), \qquad \text{with} \qquad \frac{\gamma(c)}{\gamma_0(c_0)} = \frac{1}{1-b\log(c/a+1)}. \tag{5}$$

Here γ and γ_0 are the surface tensions at concentrations c and c_0, the second being a reference concentration. The parameters a and b depend on the fluid and the medium. We refer to [40,41] for details about the scaling factor in (5).

This gives the following expressions for θ and K

$$\theta(\Psi, c) = \begin{cases} \theta_r + (\theta_s - \theta_r)\left[1/\Big(1+\big(-\alpha(\frac{1}{1-b\log(c/a+1)})\Psi\big)^n\Big)\right]^{\frac{n-1}{n}}, & \Psi \leq 0 \\ \theta_s, & \Psi > 0, \end{cases} \tag{6}$$

$$K(\theta(\Psi,c)) = \begin{cases} K_s\theta(\Psi,c)^{\frac{1}{2}}\left[1-\left(1-\theta(\Psi,c)^{\frac{n}{n-1}}\right)^{\frac{n-1}{n}}\right], & \Psi \le 0 \\ K_s, & \Psi > 0. \end{cases} \tag{7}$$

This shows that the flow component also depends on the reactive transport, implying that the model is coupled in both way.

In the following we proceed by discretizing the equations (1) and (2) in time and space. We will use common notations in functional analysis. We denote by $L^2(\Omega)$ the space of real valued, squared integrable function defined on Ω and $H^1(\Omega)$ its subspace, containing the functions having also the first order derivatives in $L^2(\Omega)$. $H_0^1(\Omega)$ is the space of functions belonging to $H^1(\Omega)$ and vanishing on $\partial\Omega$. Further, we denote by $<\cdot,\cdot>$ the $L^2(\Omega)$ scalar product (and by $\|\cdot\|$ the associated norm) or the pairing between $H1_0$ and its dual H^{-1}. Finally, by $L^2(0,T;X)$ we mean the Bochner space of functions taking values in the Banach-space X, the extension to $H^1(0,T;X)$ being straightforward.

With this we state the weak formulation of the problem related to (1) – (2):

Problem P: Find $\Psi, c \in L2(0,T;H_0^1(\Omega)) \cap H^1(0,T;H^{-1}(\Omega))$ such that

$$<\partial_t\theta(\Psi,c),\Phi_1> + <K(\theta(\Phi,c))\nabla(\Psi+z),\nabla\Phi_1> = <H_1,\Phi_1> \tag{8}$$

and

$$<\partial_t(\theta(\Psi,c)c),\Phi_2> + <K(\theta(\Psi,c))D\nabla\Psi + \mathbf{u_w}c,\nabla\Phi_2> = <H_2,\Phi_2> \tag{9}$$

hold for all $\Phi_1,\Phi_2 \in H_0^1(\Omega)$ and almost every $t \in (0,T]$.

We now combine the backward Euler method with linear Galerkin finite elements for the discretization of PRoblem P. We let $N \in \mathbb{N}$ be a strictly positive natural number and the time step $\tau := T/N$. Correspondingly, the discrete times are $t_n := n\tau$ $(n \in 0,1,\ldots,N)$. Further, we let T_h be a regular decomposition of Ω, $\overline{\Omega} = \bigcup_{T\in T_h} T$ into d-dimensional simplices, with h denoting the maximal mesh diameter. The finite element space $V_h \subset H_0^1(\Omega)$ is defined by

$$V_h := \{v_h \in H_0^1(\Omega)\ s.t.\ v_{h|T} \in \mathbb{P}_1(T),\ \text{for any } T \in T_h\}, \tag{10}$$

where $\mathbb{P}_1(T)$ denotes the space of linear polynomials on T and $v_{h|T}$ the restriction of v_h to T.

For the fully discrete counterpart of Problem P we let $n \ge 1$ be fixed and assume that $\Psi_h^{n-1}, c_h^{n-1} \in V_h$ are given. The solution pair at time t_n solves

Problem $\mathbf{P}_n$: Find $\Psi_h^n, c_h^n \in V_h$ such that for all $v_h, w_h \in V_h$ there holds

$$\begin{aligned} &<\theta(\Psi_h^n,c_h^n) - \theta(\Psi_h^{n-1},c_h^{n-1}),v_h> \\ &+\tau<K(\theta(\Psi_h^n,c_h^n))(\nabla(\Psi_h^n)+\mathbf{e_z}),\nabla v_h> = \tau<H_1,v_h> \end{aligned} \tag{11}$$

and

$$\begin{aligned} &<\theta(\Psi_h^n,c_h^n)c_h^n> - \theta(\Psi_h^{n-1},c_h^{n-1})c_h^{n-1}),w_h> \\ &+\tau<D\nabla\Psi_h + \mathbf{u_w^{n-1}}c_h^n,\nabla w_h> = \tau<H_2,w_h>. \end{aligned} \tag{12}$$

$\mathbf{e_z}$ denotes the unit vector in the direction opposite to gravity.

Remark 1 Observe that $\mathbf{u_w^{n-1}}$ appears in the convective term in (12). This choice is made for the ease of presentation. Nevertheless, all calculations carried out in this paper were doubled by ones where $\mathbf{u_w^n}$ has replaced $\mathbf{u_w^{n-1}}$. The differences in the results were marginal.

Observe that Problem P_n is a coupling system of two elliptic, nonlinear equations. In the following we discuss different iterative schemes for solving this system.

2.1 Iterative linearization schemes

We discuss monolithic and splitting approaches for solving Problem P_n, combined with either the Newton-method, or the modified Picard [11] or the *L*-scheme [33,29]. In the following the index n always refers to the time step, whereas j denotes the iteration index. As a rule, the iterations start with the solution at the last time, t_{n-1}.

In the monolithic approach one solves the two equations of the system (11)-(12) at once, and combined with a linearization method. Formally, this becomes

Problem PMon$_{n,j+1}$: Find $\Psi^{n,j+1}$ and $c^{n,j+1}$ such that

$$\begin{cases} F_1^{lin}(\Psi^{n,j+1}, c^{n,j+1}) = 0, \\ F_2^{lin}(\Psi^{n,j+1}, c^{n,j+1}) = 0. \end{cases} \tag{13}$$

F_k^{Lin} is a linearization of the expression F_k ($k = 1,2$) appearing in the system (11)-(12). Depending on the used linearization technique, one speaks about a monolithic-Newton scheme (Mon-Newton), or monolithic-Picard (Mon-Picard) or monolithic-*L*-scheme (Mon-LS). These three schemes will be presented in detail below.

In the iterative splitting approach one solves each equation separately and then iterates between these using the results obtained previously. We distinguish between two main splitting ways: the nonlinear slitting and the alternate splitting. This is schematized in Figure 1 and Figure 2 respectively. The former becomes

Problem PNonLinS$_{n,j+1}$: Find $\Psi^{n,j+1}$ and $c^{n,j+1}$ such that

$$\begin{cases} F_1(\Psi^{n,j+1}, c^{n,j}) = 0, \text{ followed by} \\ F_2(\Psi^{n,j+1}, c^{n,j+1}) = 0. \end{cases} \tag{14}$$

For the linearization of F_1 and F_2 one can use one of the three linearization techniques mentioned before. In contrast, in the alternate splitting one performs only one linearization step per iteration, see also Figure 2. The alternate splitting scheme becomes

Problem PAltS$_{n,j+1}$: Find $\Psi^{n,j+1}$ and $c^{n,j+1}$ such that

$$\begin{cases} F_1^{lin}(\Psi^{n,j+1}, c^{n,j}) = 0, \text{ followed by} \\ F_2^{lin}(\Psi^{n,j+1}, c^{n,j+1}) = 0. \end{cases} \tag{15}$$

Depending which linearization is used, one speaks about alternate splitting Newton (AltS-NE) or alternate splitting *L*-scheme (AltS-LS). Both schemes are presented in detail below.

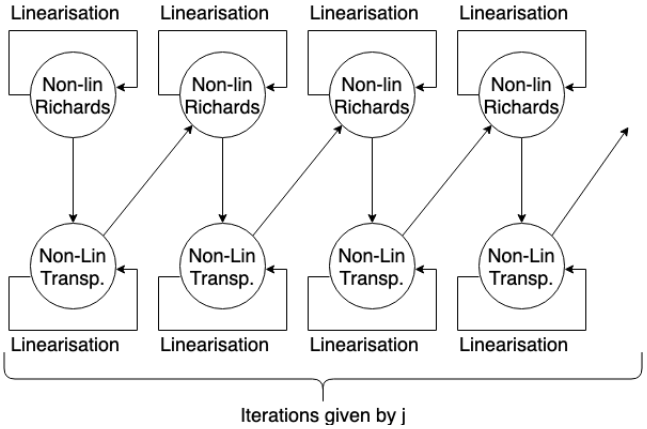

Fig. 1: The non-linear splitting approach

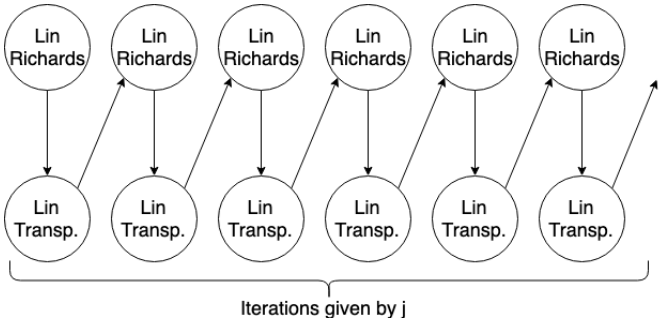

Fig. 2: The alternate splitting approach

2.1.1 The monolithic Newton method (Mon-Newton)

We recall that Newton scheme is quadratically, but only locally convergent. The monolithic Newton method applied to (11)-(12) gives

Problem PMon-Newton$_{n,j+1}$: Let $\Psi_h^{n-1}, c^{n-1}, \Psi_h^{n,j}, c_h^{n,j} \in V_h$ be given, find $\Psi_h^{n,j+1}, c_h^{n,j+1} \in V_h$ such that for all $v_h, w_h \in V_h$ one has

$$\begin{aligned} &< \theta(\Psi_h^{n,j}, c_h^{n,j}) - \theta(\Psi_h^{n-1}, c_h^{n-1}), v_h > + < \frac{\partial \theta}{\partial \Psi}(\Psi_h^{n,j}, c_h^{n,j})(\Psi_h^{n,j+1} - \Psi_h^{n,j}), v_h > \\ &\qquad + \tau < K(\theta(\Psi_h^{n,j}, c_h^{n,j}))(\nabla(\Psi_h^{n,j+1}) + \mathbf{e_z}), \nabla v_h > \\ &+ \tau < K'(\theta(\Psi_h^{n,j}, c_h^{n,j}))(\nabla(\Psi_h^{n,j+1}) + \mathbf{e_z})(\Psi_h^{n,j+1} - \Psi_h^{n,j}), \nabla v_h > = \tau < H, v_h > \end{aligned} \tag{16}$$

and

$$\begin{aligned} &< \theta(\Psi_h^{n,j}, c_h^{n,j}) c_h^{n,j+1} - \theta(\Psi_h^{n-1}, c_h^{n-1}) c_h^{n-1}), w_h > \\ &+ < \frac{\partial \theta}{\partial c}(\Psi_h^{n,j}, c_h^{n,j})(c_h^{n,j+1} - c_h^{n,j}), v_h > \\ &+ \tau < D \nabla c_h^{n,j+1} + \mathbf{u_w^{n-1}} c_h^{n,j+1}, \nabla w_h > = \ \tau < H_c, w_h > . \end{aligned} \tag{17}$$

2.1.2 The monolithic Picard (Mon-Picard)

The modified Picard method was initially proposed by Celia [11] for the Richards equation. It is similar to the Newton method in dealing with the nonlinearity in the saturation, but not in the permeability. Being a modification of the Newton method, modified Picard method is only linearly convergent [36]. The monolithic Picard method applied to (11)-(12) becomes

Problem PMon-Picard$_{n,j+1}$: Let $\Psi_h^{n-1}, c_h^{n-1}, \Psi_h^{n,j}, c_h^{n,j} \in V_h$ be given, find $\Psi_h^{n,j+1}, c_h^{n,j+1} \in V_h$ such that for all $v_h, w_h \in V_h$ one has

$$\begin{aligned} &< \theta(\Psi_h^{n,j}, c_h^{n,j}) - \theta(\Psi_h^{n-1}, c_h^{n-1}), v_h > \\ &+ < \frac{\partial \theta}{\partial \Psi}(\Psi_h^{n,j}, c_h^{n,j})(\Psi_h^{n,j+1} - \Psi_h^{n,j}), v_h > \\ &+ \tau < K(\theta(\Psi_h^{n,j}, c_h^{n,j}))(\nabla(\Psi_h^{n,j+1}) + \mathbf{e_z}), \nabla v_h > = \ \tau < H, v_h > \end{aligned} \tag{18}$$

and

$$\begin{aligned} &< \theta(\Psi_h^{n,j}, c_h^{n,j}) c_h^{n,j+1} - \theta(\Psi_h^{n-1}, c_h^{n-1}) c_h^{n-1}), w_h > \\ &+ < \frac{\partial \theta}{\partial c}(\Psi_h^{n,j}, c_h^{n,j})(c_h^{n,j+1} - c_h^{n,j}), w_h > \\ &+ \tau < D \nabla c_h^{n,j+1} + \mathbf{u_w^{n-1}} c_h^{n,j+1}, \nabla w_h > = \ \tau < H_c, w_h > . \end{aligned} \tag{19}$$

The equations (18) and (19) have been expressed as functions of only the unknown pressure $\Psi_h^{n,j+1}$ and concentration $c_h^{n,j+1}$, respectively. To achieve this, in the former we used only the derivative of θ with respect to Ψ and only the derivative of θ with respect to c in the latter.

Alternatively, both of the partial derivatives can be involved in the formulation,

$$\begin{aligned} \theta(\Psi_h^{n,j+1}, c_h^{n,j+1}) \to \theta(\Psi_h^{n,j}, c_h^{n,j}) &+ \left(\frac{\partial \theta}{\partial \Psi}\right)(\Psi_h^{n,j}, c_h^{n,j})(\Psi_h^{n,j+1} - \Psi_h^{n,j}) \\ &+ \left(\frac{\partial \theta}{\partial c}\right)(\Psi_h^{n,j}, c_h^{n,j})(c_h^{n,j+1} - c_h^{n,j}). \end{aligned} \tag{20}$$

2.1.3 The monolithic L-scheme (Mon-LS)

The monolithic L-scheme for solving (8–9) becomes

Problem PMon-LS$_{n,j+1}$: Let $\Psi_h^{n-1}, \Psi_h^{n,j}, c_h^{n-1}, c_h^{n,j} \in V_h$ be given and with $L_1, L_2 > 0$ large enough (as sepcified below), find $\Psi_h^{n,j+1}, c_h^{n,j+1} \in V_h$ s.t. for all $v_h, w_h \in V_h$

$$\begin{aligned} &< \theta(\Psi_h^{n,j}, c_h^{n,j}) - \theta(\Psi_h^{n-1}, c_h^{n-1}), v_h > + L_1 < \Psi_h^{n,j+1} - \Psi_h^{n,j}, v_h > \\ &\tau < K(\theta(\Psi_h^{n,j}, c_h^{n,j}))(\nabla(\Psi_h^{n,j+1}) + \mathbf{e_z}), \nabla v_h > = \tau < H, v_h >, \qquad \text{and} \end{aligned} \tag{21}$$

$$\begin{aligned} &< \theta(\Psi_h^{n,j}, c_h^{n,j}) c_h^{n,j+1} - \theta(\Psi_h^{n-1}, c_h^{n-1}) c_h^{n-1}), w_h > \\ &\quad + L_2 < c_h^{n,j+1} - c_h^{n,j}, w_h > + \tau < D\nabla c + \mathbf{u_w^{n-1}} c_h^{n,j+1}, \nabla w_h > \\ &\qquad = \tau < H_c, w_h > . \end{aligned} \tag{22}$$

L_1 and L_2 are free to be chosen parameters but should be large enough to ensure the convergence of the scheme, see Sec. 3. In practice, the values of L_1, L_2 are connected to $\max_{\Psi} \left\| \frac{\partial \theta}{\partial \Psi} \right\|, \max_{c} \left\| \frac{\partial \theta}{\partial c} \right\|$.

The L-scheme does not involve the computations of derivatives, and the linear systems to be solved within each iteration are better conditioned compared to the ones given by Newton or Picard method (see [29]). Moreover, this scheme is (linearly) convergent for any initial guess for the iteration.

2.1.4 The non-linear splitting approach (NonLinS)

The non-linear splitting approach for solving (8–9) becomes

Problem PNonLinS$_{n,j+1}$: Let $\Psi_h^{n-1}, c^{n-1}, \Psi_h^{n,j}, c_h^{n,j} \in V_h$ be given, find $\Psi_h^{n,j+1} \in V_h$ s.t.

$$\begin{aligned} &< \theta(\Psi_h^{n,j+1}, c_h^{n,j}) - \theta(\Psi_h^{n-1}, c_h^{n-1}), v_h > \\ &+ \tau < K(\theta(\Psi_h^{n,j}, c_h^{n,j}))(\nabla(\Psi_h^{n,j+1}) + \mathbf{e_z}), \nabla v_h > = \tau < H, v_h > \end{aligned} \tag{23}$$

holds true for all $v_h \in V_h$. Then, with $\Psi_h^{n,j+1}$ obtained, find $c_h^{n,j+1} \in V_h$ such that for all $w_h \in V_h$ it holds

$$\begin{aligned} &< \theta(\Psi_h^{n,j+1}, c_h^{n,j+1}) c_h^{n,j+1} - \theta(\Psi_h^{n-1}, c_h^{n-1}) c_h^{n-1}), w_h > + \tau < D\nabla c_h^{n,j+1} \\ &\qquad + \mathbf{u_w^{n-1}} c_h^{n,j+1}, \nabla w_h > = \ \tau < H_c, w_h > . \end{aligned} \tag{24}$$

As for the monolithic schemes, one can apply the different linear iterative schemes to obtain fully linear versions of the splitting approach. This is done first to solve (23) and, once a solution to (23) is available, this is employed in the linearization of (24).

2.1.5 The alternate Newton method (AltS-Newton)

In the alternate Newton method applied to (11)-(12) one solves

Problem PAltS-Newton$_{n,j+1}$: Let $\Psi_h^{n-1}, c^{n-1}, \Psi_h^{n,j}, c_h^{n,j} \in V_h$ be given, find $\Psi_h^{n,j+1} \in V_h$ s.t.

$$\begin{aligned} &< \theta(\Psi_h^{n,j}, c_h^{n,j}) - \theta(\Psi_h^{n-1}, c_h^{n-1}), v_h > \\ + &< \theta'(\Psi_h^{n,j}, c_h^{n,j})(\Psi_h^{n,j+1} - \Psi_h^{n,j}), v_h > + \tau < K(\theta(\Psi_h^{n,j}, c_h^{n,j}))(\nabla(\Psi_h^{n,j+1}) \\ &+ \mathbf{e_z}), \nabla v_h > + \tau < K'(\theta(\Psi_h^{n,j}, c_h^{n,j}))(\nabla(\Psi_h^{n,j+1}) \\ &+ \mathbf{e_z})(\Psi_h^{n,j+1} - \Psi_h^{n,j}), \nabla v_h >= \tau < H, v_h > \end{aligned} \tag{25}$$

holds true for all $v_h \in V_h$. Then, with $\Psi_h^{n,j+1}$ obtained above, find $c_h^{n,j+1} \in V_h$ such that for all $w_h \in V_h$ one has

$$\begin{aligned} &< \theta(\Psi_h^{n,j+1}, c_h^{n,j}) c_h^{n,j+1} - \theta(\Psi_h^{n-1}, c_h^{n-1}) c_h^{n-1}), w_h > \\ + &< \theta'(\Psi_h^{n,j+1}, c_h^{n,j})(c_h^{n,j+1} - c_h^{n,j}), v_h > + \tau < D \nabla c_h^{n,j+1} \\ &+ \mathbf{u_w^{n-1}} c_h^{n,j+1}, \nabla w_h > = \tau < H_c, w_h > . \end{aligned} \tag{26}$$

2.1.6 The alternate Picard (AltS-Picard)

The alternate Picard method applied to (11)-(12) becomes

Problem PAltS-Picard$_{n,j+1}$: Let $\Psi_h^{n-1}, c^{n-1}, \Psi_h^{n,j}, c_h^{n,j} \in V_h$ be given, find $\Psi_h^{n,j+1} \in V_h$ s.t.

$$\begin{aligned} &< \theta(\Psi_h^{n,j}, c_h^{n,j}) - \theta(\Psi_h^{n-1}, c_h^{n-1}), v_h > \\ &+ < \frac{\partial \theta}{\partial \Psi}(\Psi_h^{n,j}, c_h^{n,j})(\Psi_h^{n,j+1} - \Psi_h^{n,j}), v_h > \\ + \tau &< K(\theta(\Psi_h^{n,j}, c_h^{n,j}))(\nabla(\Psi_h^{n,j+1}) + \mathbf{e_z}), \nabla v_h > = \tau < H, v_h > \end{aligned} \tag{27}$$

hold true for all $v_h \in V_h$. Then, with $\Psi_h^{n,j+1}$ obtained above, find $c_h^{n,j+1} \in V_h$ such that for all $w_h \in V_h$ one has

$$\begin{aligned} &< \theta(\Psi_h^{n,j+1}, c_h^{n,j}) c_h^{n,j+1} - \theta(\Psi_h^{n-1}, c_h^{n-1}) c_h^{n-1}), w_h > \\ &+ < \frac{\partial \theta}{\partial c}(\Psi_h^{n,j+1}, c_h^{n,j})(c_h^{n,j+1} - c_h^{n,j}), w_h > \\ + \tau &< D \nabla c_h^{n,j+1} + \mathbf{u_w^{n-1}} c_h^{n,j+1}, \nabla w_h > = \tau < H_c, w_h > . \end{aligned} \tag{28}$$

2.1.7 The alternate L-scheme (AltS-LS)

The alternate L-scheme for solving (8–9) becomes

Problem PAltS-LS$_{n,j+1}$: Let $\Psi_h^{n-1}, c^{n-1}, \Psi_h^{n,j}, c_h^{n,j} \in V_h$ be given, find $\Psi_h^{n,j+1} \in V_h$ s.t.

$$\begin{aligned} &< \theta(\Psi_h^{n,j}, c_h^{n,j}) - \theta(\Psi_h^{n-1}, c_h^{n-1}), v_h > + L_1 < \Psi_h^{n,j+1} - \Psi_h^{n,j}, v_h > \\ &\tau < K(\theta(\Psi_h^{n,j}, c_h^{n,j}))(\nabla(\Psi_h^{n,j+1}) + \mathbf{e_z}), \nabla v_h > = \tau < H, v_h > \end{aligned} \tag{29}$$

hold true for all $v_h \in V_h$. Then, with $\Psi_h^{n,j+1}$ obtained above, find $c_h^{n,j+1} \in V_h$ such that for all $w_h \in V_h$ one has

$$\begin{aligned} &< \theta(\Psi_h^{n,j+1}, c_h^{n,j}) c_h^{n,j+1} - \theta(\Psi_h^{n-1}, c_h^{n-1}) c_h^{n-1}), w_h > \\ &+L_2 < c_h^{n,j+1} - c_h^{n,j}, w_h > + \tau < D\nabla c + \mathbf{u_w^{n-1}} c_h^{n,j+1}, \nabla w_h > \\ &= \tau < H_c, w_h > . \end{aligned} \tag{30}$$

Remark 2 (Stopping criterion) For either monolithic or splitting schemes, one stops the iteration process whenever

$$\left\| \Psi_h^{n,j+1} - \Psi_h^{n,j} \right\| \leq \varepsilon_1, \text{ and } \left\| c_h^{n,j+1} - c_h^{n,j} \right\| \leq \varepsilon_2,$$

where $\varepsilon_1, \varepsilon_2$ are small numbers. Here we took 10^{-07} or 10^{-08}.

3 Convergence analysis

In this section we analyse the convergence of the monolithic *L*-scheme introduced through Problem PMon-LS$_{n,j+1}$. We restrict the analysis to this iteration, but mention that the convergence analysis for the other (monolithic or splitting) schemes introduced above, can be done in a similar fashion. We start by defining the errors

$$e_\Psi^{j+1} := \Psi_h^{n,j+1} - \Psi_h^{n,j} \text{ and } e_c^{j+1} := c_h^{n,j+1} - c_h^{n,j}, \tag{31}$$

obtained at iteration $j+1$. The scheme is convergent if both errors vanish when $j \to \infty$.

The convergence is obtained under the following assumptions:

(A1) There exist $\alpha_\Psi > 0$ and $\alpha_c \geq 0$ such that for any $\Psi_1, \Psi_2 \in \mathbb{R}$ and $c_1, c_2 \in \mathbb{R}_+$

$$\begin{aligned} &< \theta(\Psi_1, c_1) - \theta(\Psi_2, c_2), \Psi_1 - \Psi_2 > + < c_1 \theta(\Psi_1, c_1) - c_2 \theta(\Psi_2, c_2), c_1 - c_2 > \\ &\geq \alpha_\Psi \left\| \theta(\Psi_1, c_1) - \theta(\Psi_2, c_2) \right\|^2 + \alpha_c \left\| \Psi_1 - \Psi_2 \right\|^2. \end{aligned} \tag{32}$$

Furthermore, there exist two constants $\theta_m \geq 0$ and $\theta_M < \infty$ such that $\theta_m \leq \theta \leq \theta_M$.

(A2) The function $K(\theta(\cdot,\cdot))$ is Lipschitz continuous, with respect to both variables, and there exist two constants K_m and K_M such that $0 \leq K_m \leq K \leq K_M < \infty$.

(A3) There exist $M_u, M_\Psi, M_c \geq 0$ such that $\|\mathbf{u_w^n}\|_{L^\infty} \leq M_u$, $\|\nabla \Psi^n\|_{L^\infty} \leq M_\Psi$ and $\|c^n\|_{L^\infty} \leq M_c$ for all $n \in \mathbb{N}$.

Remark 3 (A2) is satisfied in most realistic situations. (A3) is a pure technical one, being satisfied when data is sufficiently regular, which is assumed to be the case for the present analysis. The inequality (32) in (A1) is a coercivity assumption. It is in particular satisfied if Θ only depends on Ψ, and for common relationships $\Theta - -\Psi$ encountered in the engineering literature.

Theorem 1 *Let $n \in \{1, 2, \ldots N\}$ be given and assume (A1)-(A3) be satisfied. If the time step is small enough (see* (42) *below), the monolithic L-scheme in (29) and (30) is linearly convergent for any L_1 and L_2 satisfying* (41)*.*

Proof We follow the ideas in [33,29] and start by subtracting (11) from (29) to obtain the error equation

$$\begin{aligned} &< \theta_h^{n,j}-\theta_h^n, v_h > + L_1 < \Psi_h^{n,j+1}-\Psi_h^{n,j}, v_h > \\ &+\tau < K_h^{n,j}\nabla e_\Psi^{n,j+1}, \nabla v_h > + \tau < (K^{n,j}-K^n)\nabla \Psi_h^{n,j+1}, \nabla v_h > \\ &+\tau < (K^{n,j}-K^n)\mathbf{e_z}, \nabla v_h >= 0. \end{aligned} \tag{33}$$

Testing now the above equation with $v_h = e_\Psi^{j+1}$, one obtains

$$\begin{aligned} &< \theta_h^{n,j}-\theta_h^n, e_\Psi^{j+1} > + L_1 < e_\Psi^{j+1}-e_\Psi^j, e_\Psi^{j+1} > \\ &+\tau < K^{n,j}\nabla e_\Psi^{n,j+1}, \nabla e_\Psi^{j+1} > + \tau < (K_h^{n,j}-K_h^n)\nabla \Psi_h^{n,j+1}, \nabla e_\Psi^{j+1} > \\ &+\tau < (K_h^{n,j}-K_h^n)\mathbf{e_z}, \nabla e_\Psi^{j+1} >= 0. \end{aligned} \tag{34}$$

By (A2) and after some algebraic manipulations we further get

$$\begin{aligned} &< \theta_h^{n,j}-\theta_h^n, e_\Psi^j > + \frac{L_1}{2}\left\|e_\Psi^{j+1}\right\|^2 + \frac{L_1}{2}\left\|e_\Psi^{j+1}-e_\Psi^j\right\|^2 \\ &+\tau K_m \left\|\nabla e_\Psi^{j+1}\right\|^2 \leq \frac{L_1}{2}\left\|e_\Psi^j\right\|^2 - < \theta_h^{n,j}-\theta_h^n, e_\Psi^{j+1}-e_\Psi^j > \\ &-\tau < (K_h^{n,j}-K_h^n)\nabla \Psi_h^{n,j+1}, \nabla e_\Psi^{j+1} > -\tau < (K_h^{n,j}-K_h^n)\mathbf{e_z}, \nabla e_\Psi^{j+1} > . \end{aligned} \tag{35}$$

Using now (A1), (A3), the Lipschitz continuity of K and twice the Young and Cauchy-Schwarz inequalities, for any $\delta_0 > 0$ and $\delta_1 > 0$, from (35) one obtains

$$\begin{aligned} &< \theta_h^{n,j}-\theta_h^n, e_\Psi^j > + \frac{L_1}{2}\left\|e_\Psi^{j+1}\right\|^2 + \frac{L_1}{2}\left\|e_\Psi^{j+1}-e_\Psi^j\right\|^2 \\ &+\tau K_m \left\|\nabla e_\Psi^{j+1}\right\|^2 \leq \frac{L_1}{2}\left\|e_\Psi^j\right\|^2 + \frac{\delta_0}{2}\left\|\theta_h^{n,j}-\theta_h^n\right\|^2 + \frac{1}{2\delta_0}\left\|e_\Psi^{j+1}-e_\Psi^j\right\|^2 \\ &+\frac{\tau(M_\Psi^2+1)L_k^2}{2\delta_1}\left\|\theta_h^{n,j}-\theta_h^n\right\|^2 + \tau\delta_1\left\|\nabla e_\Psi^{j+1}\right\|^2. \end{aligned} \tag{36}$$

Similarly, subtracting (12) from (30) and choosing $w_h = e_c^{j+1}$ in the resulting one gets

$$\begin{aligned} &< c_h^{n,j+1}\theta_h^{n,j} - c_h^n\theta_h^n, e_c^{j+1} > + L_2 < e_c^{j+1}-e_c^j, e_c^{j+1} > \\ &+\tau < D\nabla e_c^{j+1} + \mathbf{u_w^{n-1}} e_c^{j+1}, \nabla e_c^{j+1} >= 0. \end{aligned} \tag{37}$$

This can be rewritten as

$$\begin{aligned} &< c_h^{n,j}\theta_h^{n,j} - c^n\theta_h^n, e_c^j > + < \theta_h^{n,j}e_c^{j+1}, e_c^{j+1} > + \frac{L_2}{2}\left\|e_c^{j+1}\right\|^2 \\ &+\frac{L_2}{2}\left\|e_c^{j+1}-e_c^j\right\|^2 + \tau D < \nabla e_c^{j+1}, \nabla e_c^{j+1} >= \frac{L_2}{2}\left\|e_c^j\right\|^2 \\ &+ < \theta_h^n c_h^n - \theta_h^{n,j}c_h^{n,j}, e_c^{j+1}-e_c^j > -\tau < \mathbf{u_w^{n-1}} e_c^{j+1}, \nabla e_c^{j+1} > . \end{aligned} \tag{38}$$

Using again (A1), (A3) and the Cauchy-Schwarz and Young inequalities, from (38) it follows that for any $\delta_2, \delta_3, \delta_4 > 0$ one has

$$\begin{aligned} < c_h^{n,j}\theta_h^{n,j} - c_h^n\theta_h^n, e_c^j > &+ \theta_m \left\|e_c^{j+1}\right\|^2 + \frac{L_2}{2}\left\|e_c^{j+1}\right\|^2 + \frac{L_2}{2}\left\|e_c^{j+1} - e_c^j\right\|^2 \\ &+ \tau D\left\|\nabla e_c^{j+1}\right\|^2 \leq \frac{L_2}{2}\left\|e_c^j\right\|^2 + \frac{\delta_2}{2}\left\|\theta_h^n - \theta_h^{n,j}\right\|^2 + \frac{\delta_3}{2}\left\|e_c^j\right\|^2 \\ &+ (\frac{M_c^2}{2\delta_2} + \frac{\theta_M^2}{2\delta_3})\left\|e_c^{j+1} - e_c^j\right\|^2 + \tau\frac{M_u^2}{2\delta_4}\left\|e_c^{j+1}\right\|^2 + \tau\frac{\delta_4}{2}\left\|\nabla e_c^{j+1}\right\|^2. \end{aligned} \tag{39}$$

Summing adding (36) to (39) and using (A1) one gets

$$\begin{aligned} \alpha_\Psi \left\|\theta_h^n - \theta_h^{n,j}\right\|^2 &+ \frac{L_1}{2}\left\|e_\Psi^{j+1}\right\|^2 + \frac{L_1}{2}\left\|e_\Psi^{j+1} - e_\Psi^j\right\|^2 + \tau K_m\left\|\nabla e_\Psi^{j+1}\right\|^2 \\ &+ \alpha_c\left\|e_c^j\right\|^2 + \theta_m\left\|e_c^{j+1}\right\|^2 + \frac{L_2}{2}\left\|e_c^{j+1}\right\|^2 + \frac{L_2}{2}\left\|e_c^{j+1} - e_c^j\right\|^2 \\ &+ \tau D\left\|\nabla e_c^{j+1}\right\|^2 \leq \frac{L_1}{2}\left\|e_\Psi^j\right\|^2 + (\frac{\delta_0}{2} + \frac{\tau(M_\Psi^2+1)L_k^2}{2\delta_1} \\ &+ \frac{\delta_2}{2})\left\|\theta_h^{n,j} - \theta_h^n\right\|^2 + \frac{1}{2\delta_0}\left\|e_\Psi^{j+1} - e_\Psi^j\right\|^2 + \tau\delta_1\left\|\nabla e_\Psi^{j+1}\right\|^2 + \frac{L_2}{2}\left\|e_c^j\right\|^2 \\ &+ \frac{\delta_3}{2}\left\|e_c^j\right\|^2 + (\frac{M_c^2}{2\delta_2} + \frac{\theta_M^2}{2\delta_3})\left\|e_c^{j+1} - e_c^j\right\|^2 + \tau\frac{M_u^2}{2\delta_4}\left\|e_c^{j+1}\right\|^2 \\ &+ \tau\frac{\delta_4}{2}\left\|\nabla e_c^{j+1}\right\|^2. \end{aligned} \tag{40}$$

Choosing $\delta_0 = \delta_2 = \dfrac{\alpha_\Psi}{2}$, $\delta_1 = \dfrac{K_m}{2}$, $\delta_3 = \theta_m$ and $\delta_4 = \dfrac{D}{2}$ in (40), and assuming that

$$L_1 \geq \frac{2}{\alpha_\Psi} \text{ and } L_2 \geq \frac{2M_c^2}{\alpha_\Psi} + \frac{\theta_M^2}{\theta_m}, \tag{41}$$

and the time step τ satisfies the mild conditions

$$\alpha_\Psi - 2\tau\frac{\tau(M_\Psi^2+1)L_k^2}{K_m} \geq 0 \quad \text{and} \quad \theta_m + 2\alpha_c + \frac{\tau D}{C_\Omega} - \frac{2\tau M_u^2}{D} \geq 0, \tag{42}$$

where C_Ω denotes the Poincare constant, then we obtain

$$\begin{aligned} \frac{L_1}{2}\left\|e_\Psi^{j+1}\right\|^2 &+ \tau\frac{K_m}{2}\left\|\nabla e_\Psi^{j+1}\right\|^2 + (\frac{L_2}{2} + \theta_m - \tau\frac{M_u^2}{D})\left\|e_c^{j+1}\right\|^2 \\ &+ \tau\frac{D}{2}\left\|\nabla e_c^{j+1}\right\|^2 \leq \frac{L_1}{2}\left\|e_\Psi^j\right\|^2 + (\frac{L_2}{2} + \frac{\theta_m}{2} - \alpha_c)\left\|e_c^j\right\|^2. \end{aligned} \tag{43}$$

Finally, by using the Poincare inequality two times we get from (43)

$$\begin{aligned} (L_1 + \tau\frac{K_m}{C_\Omega})\left\|e_\Psi^{j+1}\right\|^2 &+ (L_2 + 2\theta_m + \tau\frac{D}{C_\Omega} - 2\tau\frac{M_u^2}{D})\left\|e_c^{j+1}\right\|^2 \\ &\leq L_1\left\|e_\Psi^j\right\|^2 + (L_2 + \theta_m - 2\alpha_c)\left\|e_c^j\right\|^2. \end{aligned} \tag{44}$$

From (42), (44) implies that the errors are contracting and therefore the monolithic L-scheme (29) - (30) is convergent.

Remark 4 The convergence rate resulting from (44) do not depend on the spatial mesh size. Also observe that this convergence is obtained for any initial guess. Based on this, the method is globallly convergent, which is in contrast to the Newton or (modified) Picard schemes, converging only locally. It can be observed that, the larger the time step, the smaller the constants L_1 and L_2 are, resulting in a faster convergence. For small steps instead the convergence rate can approach 1. On the other hand, if the time step is small enough, one may reach the regime where the Newton scheme becomes convergent (see [36]). Alternatively, one may first perform a number of L-scheme iterations, and use the resulting as an initial guess for the Newton scheme (see [29]), or consider the modified L-scheme in [30]. In either situations, the convergence behavior was much improved.

Remark 5 The convergence of the modified Picard and Newton method applied to the Richards equation has been already proved in [36]. Such results can be extended to the coupled problems considered here.

4 Numerical examples

In this section we consider four test cases for the proposed linearization schemes, inspired by the literature [29,26]. The schemes have been implemented in the open source software package MRST [28], an open source toolbox based on Matlab, in which multiple solvers and models regarding flows in porous media are incorporated.

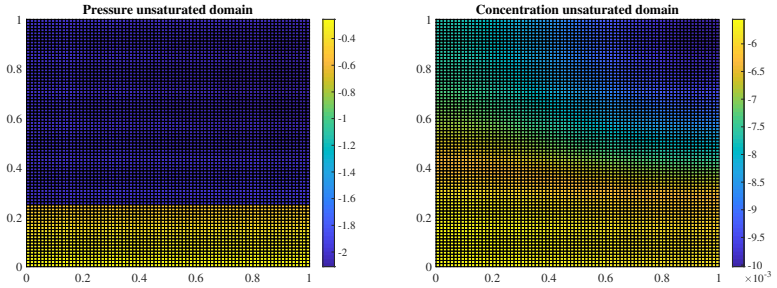

(a) Pressure profile at T = 1 (b) Concentration profile at T = 1

Fig. 3: Example 1A: pressure and concentration profiles at the final time $T = 1$. The simulations were performed with $dx = 1/80$ and $\tau = 1/10$

Example 1A: flow and transport in strictly unsaturated media

We start our numerical studies with a manufactured problem admitting an analytical solution [29]. The unit square Ω is divided into two sub-domains: Ω_{up} and Ω_{down}.

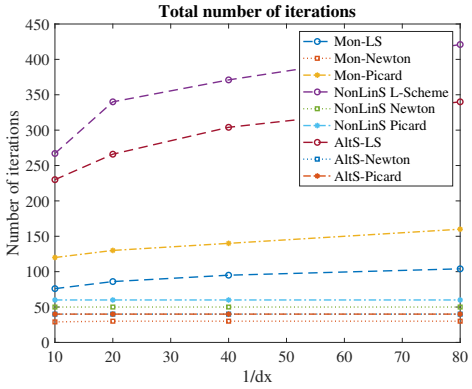

Fig. 4: Total numbers of iterations

T_{max}	10 h
Ω	$[0,1]\times[0,1]$
L_Ψ	.1
L_c	.005
Van Genuchten parameters	
θ_s	.42
θ_r	.0026
n	2.9
α	.95
a	.044
b	.4745
Surface tension parameters	
ζ	2.4901
$\sigma 0$	73 mN/m
K_s	.12 cm/min
D_0	6.0e-04
Accuracy requirement	
ε	e-07

Table 1: Parameters involved in all the examples

The two regions are defined as: $\Omega_{up} = [0,1]\times[1/4,1]$ and $\Omega_{down} = [0,1]\times[0,1/4]$. Dirichlet boundary conditions, $\Psi = -3$, and no-flow Neumann boundary conditions are imposed on $\Gamma_D = [0,1]\times 1$ and $\Gamma_N = \partial\Omega/\Gamma_D$, respectively. A constant initial pressure $p^0_{up} = -2$, and a non-constant $p^0_{down} = -y - 1/4$ are defined in the upper and in the lower part of the domain, Ω_{up} and Ω_{down}. The van Genuchten parameters are presented in Table 1.

Further, for both Richards and transport equations, we have a source term, $f(x,y) = .006\cos(4/3\pi y)\sin(x)$, on Ω_{up}. No external forces or sources, are defined in the lower region, i.e. $f = 0$ on Ω_{down}. Finally, the initial condition for the concentration is given by $c^0 = 1$ and the boundary conditions by $c_{|\Gamma_D} = 4$.

	Monolithic		NonLinS			AltLinS		
	Newton		Newton			Newton		
				cond. #			cond. #	
dx	# iterations	condition #	# iterations	Richards	Transport	# iterations	Richards	Transport
1/10	20	511.0045	40	333.4035	5.9916	20	333.4019	5.9916
1/20	20	2.2933e+03	40	1.5040e+03	6.2079	20	1.5040e+03	6.2079
1/40	20	9.4458e+03	40	6.1312e+03	6.3234	20	6.1312e+03	6.3234
1/80	20	3.8371e+04	40	2.4774e+04	6.3816	20	2.4774e+04	6.3817
	L Scheme		L Scheme			L Scheme		
				cond. #			cond. #	
dx	# iterations	condition #	# iterations	Richards	Transport	# iterations	Richards	Transport
1/10	277	183.4223	540	177.4742	2.1356	264	177.4725	2.1356
1/20	300	812.5650	650	796.5765	2.1839	316	796.5755	2.1839
1/40	363	3.3450e+03	750	3.2584e+03	2.2092	368	3.2584e+03	2.2092
1/80	510	1.3585e+04	850	1.3191e+04	2.2220	421	1.3191e+04	2.2220
	Picard		Picard			Picard		
				cond. #			cond. #	
dx	# iterations	condition #	# iterations	Richards	Transport	# iterations	Richards	Transport
1/10	100	326.8280	40	177.4610	5.9916	20	177.4601	5.9916
1/20	110	1.4667e+03	40	796.5170	6.2079	20	796.5129	6.2079
1/40	120	6.0380e+03	40	3.2581e+03	6.3234	20	3.2581e+03	6.3234
1/80	130	2.4522e+04	40	1.3190e+04	6.3816	20	1.3190e+04	6.3817

Table 2: Example 1A: unsaturated medium, fixed $\tau = 1/10$

	Monolithic		NonLinS			AltLinS		
	Newton		Newton			Newton		
				cond. #			cond. #	
dt	# iterations	condition #	# iterations	Richards	Transport	# iterations	Richards	Transport
1/10	20	9.4458e+03	40	6.1312e+03	6.3234	20	6.1312e+03	6.3234
1/20	40	4.7275e+03	80	3.2581e+03	6.3234	40	3.2580e+03	6.3234
1/40	80	2.3677e+03	160	1.7024e+03	6.3234	80	1.7024e+03	6.3234
1/80	160	1.1876e+03	320	870.8016	6.3234	160	870.8010	6.3234
	L Scheme		L Scheme			L Scheme		
				cond. #			cond. #	
dt	# iterations	condition #	# iterations	Richards	Transport	# iterations	Richards	Transport
1/10	363	3.3450e+03	750	3.2584e+03	2.2092	368	3.2584e+03	2.2092
1/20	570	1.7540e+03	1300	1.7026e+03	2.2092	633	1.7026e+03	2.2092
1/40	1048	898.9759	2160	870.2808	2.2092	1050	870.8979	2.2092
1/80	1914	455.3332	3520	440.6573	2.2092	1700	440.8161	2.2092
	Picard		Picard			Picard		
				cond. #			cond. #	
dt	# iterations	condition #	# iterations	Richards	Transport	# iterations	Richards	Transport
1/10	120	6.0380e+03	40	3.2581e+03	6.3234	20	3.2581e+03	6.3234
1/20	220	3.0216e+03	80	1.7025e+03	6.3234	40	1.7025e+03	6.3234
1/40	400	1.5132e+03	160	870.8263	6.3234	80	870.8251	6.3234
1/80	640	758.9936	320	440.8018	6.3234	160	440.8015	6.3234

Table 3: Example 1A: unsaturated medium, fixed dx=1/40

We performed simulations using regular meshes, consisting of squares, whose sides were of length $dx = [1/10,\ 1/20,\ 1/40,\ 1/80]$. We consider also varying time steps of sizes $\tau = [1/10,\ 1/20,\ 1/40,\ 1/80]$. In Fig. 3a we are plotting the pressure and concentration profiles at the final time $T = 1$. We point out that in this first example we are always in the strictly unsaturated regime, implying that Richards equation is a regular. All the proposed iterative schemes were converging for this example. In Fig. 4 is given the total number of iterations for the different schemes.

More details regarding the total number of iterations and the condition number of the linear systems are presented in Tables 2, 3. The condition number is computed at the first iteration of each algorithm and with respect to the Euclidean norm. In Table 2, we fixed a time step $\tau = 1/10$ and we investigated different mesh sizes, precisely $dx = [1/10, 1/20, 1/40, 1/80]$. In Table 3 we use a constant $dx = 1/40$ and varying the time step sizes $\tau = [1/10, 1/20, 1/40, 1/80]$. We point out that the alternate schemes are converging much faster than the classical ones. We also remark the high differences in the condition numbers, the $L-$scheme based algorithms being much better conditioned.

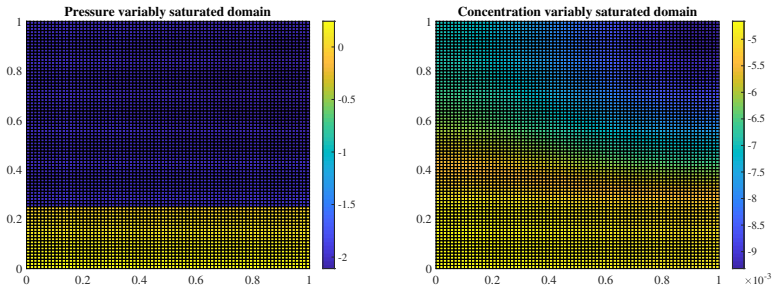

(a) Pressure profile (b) Concentration profile

Fig. 5: Example 1B: plots of pressure and concentration in the variably saturated medium, the simulations were done with $dx = 1/80$ and $dt = 1/10$

Example 1B: flow and transport in variably saturated porous media

For the second example we use the same domain, mesh sizes, boundary conditions and parameters, but we allow a saturated/unsaturated regime by changing the initial condition for the pressure. We consider a subdivision of p^0 between upper and lower regions, precisely: $p^0_{up} = -2$ and $p^0_{down} = -y + 1/4$. This new expression for p^0_{down} gives a positive pressure in the lower part of the domain (saturated region). For this example the Richards equation is now degenerate parabolic, therefore more challenging for the numerical schemes. Furthermore, we introduce this time also a reaction term $R(c)$ in the transport equation, given by $R(c) := c/(1+c)$.

At the iteration $j+1$, the term $R(c)$ is linearized in the following way:

$$R(c^{n+1,j+1}) \to \frac{1 + c^{n+1,j+1}}{c^{n+1,j}}$$

In Fig. 10a we show again the pressure and concentration profiles at the final step $T = 1$. The main differences to the previous example, i.e. Figure (3a) are in the values of the pressure. We can observe again a discontinuity in the pressure profile but, more importantly, it is evident a jump from negative to positive values. Such results were expected considering the initial pressure imposed on the domain.

In Fig. 6 are presented the total number of iterations. We remark that in this case only the $L-$scheme based algorithms are converging. It is also interesting to observe that the difference in the number of iterations between the more commonly used non-linear splitting approach (NonLinS) and alternate splitting (AltLinS) approach. The alternate method appears to be a valid alternative to the common formulation. It produces equally accurate results, requiring fewer iterations.

As for the previous example we present in the Tables 4, 5 the precise numbers of iterations and condition numbers for each algorithm implemented for different mesh diameters and time steps. Each segment $(-)$ in the tables below, implies that the method failed to converge for such particular combination of time step and space

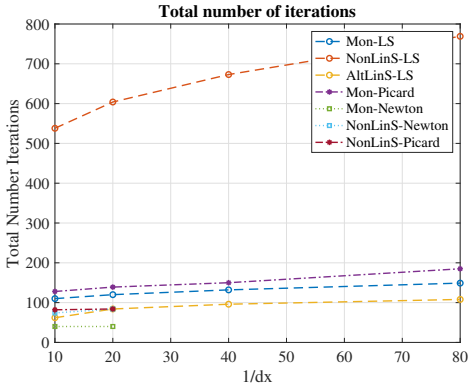

Fig. 6: Example 1B: numbers of iterations in the variably saturated porous medium

	Monolithic		NonLinS			AltLinS		
	Newton		Newton			Newton		
				cond. #			cond. #	
dx	# iterations	condition #	# iterations	Richards	Transport	# iterations	Richards	Transport
1/10	28	2.2753e+11	50	5.7734e+09	1.1251	-	5.5783e+09	1.0117
1/20	-	1.2345e+12	-	4.6521e+09	1.0126	-	.6521e+09	1.0126
1/40	-	4.5159e+12	-	5.2321e+09	1.0124	-	5.2321e+09	1.0124
1/80	-	.7232e+13	-	5.5219e+09	1.0123	-	5.5219e+09	1.0123
	L Scheme		L Scheme			L Scheme		
				cond. #			cond. #	
dx	# iterations	condition #	# iterations	Richards	Transport	# iterations	Richards	Transport
1/10	175	247.8672	440	239.2940	1.3314	264	239.8408	1.3314
1/20	314	1.0576e+03	650	1.0432e+03	1.3338	316	1.0432e+03	1.3338
1/40	352	4.2256e+03	750	4.1291e+03	1.3328	368	4.1291e+03	1.3328
1/80	408	1.6902e+04	910	1.6437e+04	1.3323	421	1.6437e+04	1.3323
	Picard		Picard			Picard		
				cond. #			cond. #	
dx	# iterations	condition #	# iterations	Richards	Transport	# iterations	Richards	Transport
1/10	-	4.5478e+11	50	5.7735e+09	1.1251	-	5.5783e+09	.0117
1/20	-	2.4690e+12	-	4.6521e+09	1.0126	-	4.6521e+09	1.0126
1/40	-	9.0318e+12	-	5.2321e+09	1.0124	-	5.2321e+09	1.0124
1/80	-	3.4465e+13	-	5.5219e+09	1.0123	-	5.5219e+09	1.0123

Table 4: Example 1B: variably saturated medium, fixed $\tau = 1/10$

mesh. As already observed in Fig. 6 the *L*-scheme based solvers are the only ones converging in all cases. Moreover, the linear systems associated with the *L*-scheme are better conditioned than the ones for Picard or Newton methods. We finally remark that, as expected, for smaller time steps the Newton and Picard schemes converges, see Table 5.

Example 2A: well in unsaturated porous media

Our next example is inspired from [26]. We consider same domain (e.g. the unit square), boundary and initial condition and parameters as in the first numerical example (1A). The medium is again strictly unsaturated. We include now, in the upper part of the domain, a well and inject water with a specific concentration of the external component. No analytical solution is available for this case. Due to the higher complexity of the problem we use more refined meshes, precisely $dx =$

	Monolithic		NonLinS			AltLinS		
	Newton		Newton			Newton		
			cond. #			cond. #		
dt	# iterations	condition #	# iterations	Richards	Transport	# iterations	Richards	Transport
1/10	-	4.5159e+12	-	5.2321e+09	1.0124	-	5.5783e+09	1.0117
1/20	-	4.5194e+12	-	2.1747e+10	1.0062	-	4.6521e+09	1.0126
1/40	80	4.5265e+12	200	1.0442 e+10	1.1325	-	5.2321e+09	1.0124
1/80	160	4.5406e+12	400	4.3494e+10	1.1325	-	5.5219e+09	1.0123
	L Scheme		L Scheme			L Scheme		
			cond. #			cond. #		
dt	# iterations	condition #	# iterations	Richards	Transport	# iterations	Richards	Transport
1/10	352	4.2256e+03	750	4.1291e+03	1.3328	368	4.1291e+03	1.3328
1/20	627	2.2518e+03	1300	2.1862e+03	1.3328	633	2.1890e+03	1.3328
1/40	1100	1.1624e+03	2160	1.1258e+03	1.3328	1050	1.1266e+03	1.3328
1/80	1900	589.7690	3520	570.6119	1.3328	1700	571.0523	1.3328
	Picard		Picard			Picard		
			cond. #			cond. #		
τ	# iterations	condition #	# iterations	Richards	Transport	# iterations	Richards	Transport
1/10	-	2.4690e+12	-	5.2321e+09	1.0124	-	5.2321e+09	1.0124
1/20	-	9.0388e+12	-	1.0442e+10	1.0062	-	1.0442e+10	1.0062
1/40	-	9.0529e+12	200	2.1748e+10	1.1325	-	2.0860e+10	1.0031
1/80	-	9.0811e+12	400	4.3494e+10	1.1325	-	4.1698e+10	1.0015

Table 5: Example 1B: variably saturated medium, fixed dx=1/40

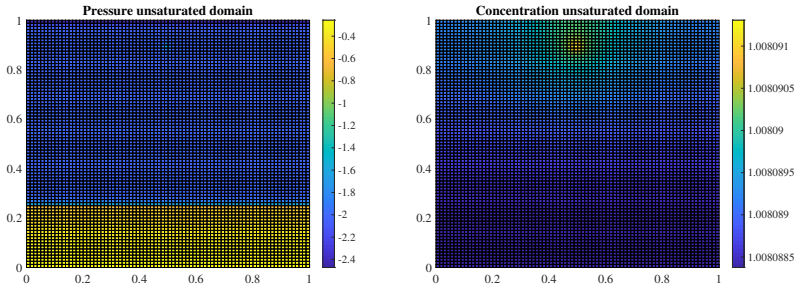

(a) Pressure profile at first time step

(b) Concentration profile at first time step

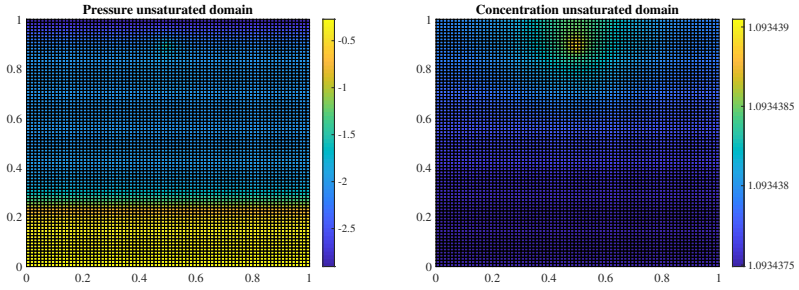

(c) Pressure profile after one day

(d) Concentration profile after one day

Fig. 7: Example 2A: plots of pressure and concentration in unsaturated medium, the simulations were done with $dx = 1/100$ and $\tau = dx$

$[1/50, 1/100, 1/150, 1/200]$. The pressure at the well is set to $p_W = -10$ and the concentration of the surfactant to $c_W = 10$.

In Fig. 7, we present the different profiles of pressure and concentration at the initial time t^0 and at final time $T = 1$ day.

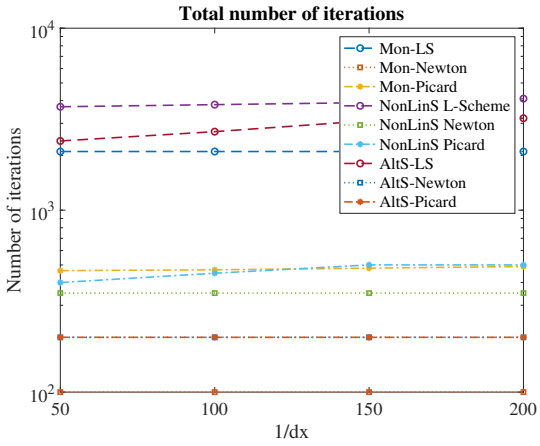

Fig. 8: Example 2A: Logarithmic plot of numbers of iterations in unsaturated porous medium

	Monolithic		NonLinS			AltLinS		
	Newton		Newton			Newton		
				cond. #			cond. #	
dx	# iterations	condition #	# iterations	Richards	Transport	# iterations	Richards	Transport
1/50	100	7.6243e+09	350	22.2624	3.3828e+09	200	22.1804	3.1779e+09
1/100	100	4.2369e+10	350	25.9419	5.2695e+10	200	31.8223	5.5839e+10
1/150	100	1.0394e+11	350	42.8667	2.8324e+11	200	33.0562	2.8324e+11
1/200	100	1.9614e+11	350	56.4999	9.1099e+11	200	42.8581	9.1662e+11
	L Scheme		L Scheme			L Scheme		
				cond. #			cond. #	
dx	# iterations	condition #	# iterations	Richards	Transport	# iterations	Richards	Transport
1/50	2100	2.7971e+09	3700	4.2830	1.6426e+09	2400	4.2489	1.4735e+09
1/100	2100	2.5556e+10	3800	5.0706	2.6387e+10	2700	5.0005	2.6331e+10
1/150	2100	7.6270e+10	3900	6.3840	1.4791e+11	3100	6.3731	1.4165e+11
1/200	2100	1.3652e+11	4100	8.1437	4.5556e+11	3200	8.2452	4.5159e+11
	Picard		Picard			Picard		
				cond. #			cond. #	
τ	# iterations	condition #	# iterations	Richards	Transport	# iterations	Richards	Transport
1/50	465	4.3612e+09	400	22.3247	1.7215e+09	200	22.1612	7.6372e+08
1/100	470	3.2796e+10	450	25.9427	2.6395e+10	200	26.0764	1.3243e+10
1/150	480	9.0401e+10	500	33.4899	1.4173e+11	200	33.0714	7.0961e+10
1/200	490	1.7576e+11	500	42.7698	4.5570e+11	200	42.737	2.2773e+11

Table 6: Example 2A: unsaturated medium, fixed $\tau = 1/50$

Once more, in Fig. 8 we compare the different solving algorithms. We study the numbers of iterations and the conditions numbers of the linearized systems. As for the first example, the media being unsaturated, the Richards equation does not degenerate and all the schemes converge. We can observe, in the Tables 6, 7, that the monolithic Newton method is the fastest, in term of numbers of iterations. We remark that the alternate splitting approach (AltLinS), once more, requires fewer iterations than the classical splitting algorithm (NonLinS) for all of the linearization schemes. The linear systems resulting by applying the L-scheme based solvers are better conditioned compared with the other solvers.

	Monolithic		NonLinS			AltLinS		
	Newton		Newton			Newton		
				cond. #			cond. #	
dt	# iterations	condition #	# iterations	Richards	Transport	# iterations	Richards	Transport
1/50	100	7.6243e+09	300	22.2624	3.3828e+09	200	22.1804	3.1779e+09
1/100	200	2.7797e+09	350	23.0671	8.0658e+08	400	22.9854	3.8663e+08
1/150	300	1.4883e+09	400	21.3871	3.8252e+08	600	21.9674	2.0727e+08
1/200	400	9.2045e+08	500	21.2462	1.9030e+08	800	21.3715	1.8499e+08
	L Scheme		L Scheme			L Scheme		
				cond. #			cond. #	
dt	# iterations	condition #	# iterations	Richards	Transport	# iterations	Richards	Transport
1/50	2100	2.7971e+09	3700	4.2830	1.6426e+09	2400	4.2489	1.4735e+09
1/100	4100	8.0703e+08	7700	4.1966	3.6673e+08	4200	4.1408	1.8802e+08
1/150	5900	3.8356e+08	11250	4.1439	1.6219e+08	5800	4.1052	8.4601e+07
1/200	7700	2.2641e+08	14600	4.0893	9.1518e+07	7200	4.0870	4.7818e+07
	Picard		Picard			Picard		
				cond. #			cond. #	
dt	# iterations	condition #	# iterations	Richards	Transport	# iterations	Richards	Transport
1/50	465	4.3612e+09	400	22.3247	1.7215e+09	200	22.1612	7.6372e+08
1/100	880	1.3673e+09	600	23.0000	1.9895e+08	400	21.5095	1.9878e+08
1/150	1300	6.6937e+08	900	22.4168	9.6242e+07	600	21.2971	8.8586e+07
1/200	1700	4.0868e+08	1200	21.2490	5.0376e+07	750	21.2490	5.0376e+07

Table 7: Example 2A: unsaturated medium, fixed dx=1/50

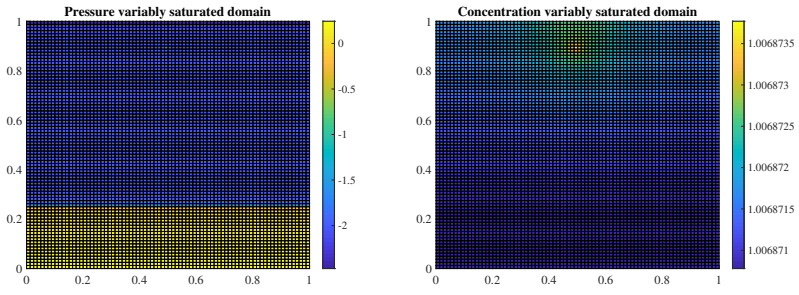

(a) Pressure profile at first time step

(b) Concentration profile at first time step

Fig. 9: Example 2B: plots of pressure and concentration in unsaturated medium, the simulations were done with $dx = 1/80$ and $\tau = dx/100$

Example 2B: well in variably saturated porous media

Our last numerical example is obtained by changing the initial condition for pressure in the example 2A. We use the same p^0 as in example 1B. The profiles of pressure and concentration at the beginning and end of the simulation, i.e. at $T = 1$ hour, are presented in Fig. 11. We can observe smaller changes, compared to the previous example, due to a smaller time interval (1 hour versus 1 day). In Fig. 11 we present the total number of iterations for the different schemes applied to example 2B. Similar to the example 1B, due to the degeneracy of the Richards equation, many of the considered schemes show convergence problems. In the Tables 8,9 we study the convergence of the schemes and the condition number of the associated linear systems. The results are very similar with the previous examples, with the L-scheme based solvers being the most robust one for all the cases and with the alternate method being faster than the classical splitting schemes.

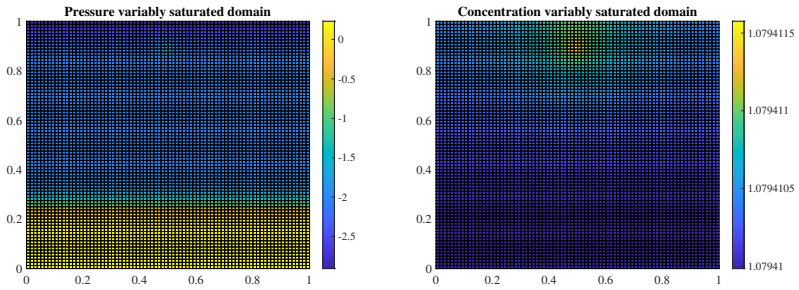

(a) Pressure profile after one hour (b) Concentration profile after one hour

Fig. 10: Example 2B: pressure and concentration profiles after one hour. The simulations were done with $dx = 1/80$ and $\tau = dx/100$

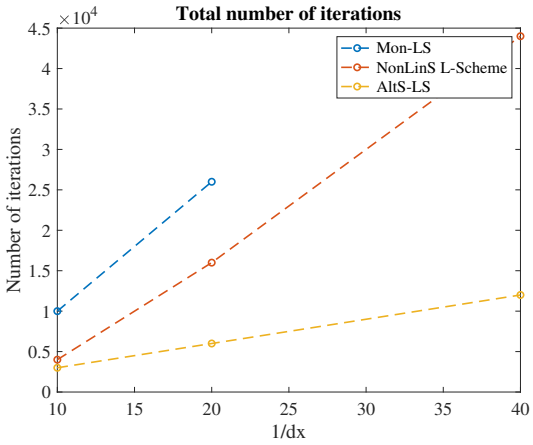

Fig. 11: Example 2B: total number of iterations for different algorithms

	Monolithic		NonLinS			AltLinS		
	Newton		Newton			Newton		
				cond. #			cond. #	
dx	# iterations	condition #	# iterations	Richards	Transport	# iterations	Richards	Transport
1/10	-	2.2435e+10	-	20.9641	3.2267e+08	-	20.9795	3.2267e+08
1/20	-	1.2309e+11	-	20.9642	5.3778e+08	-	20.9800	5.3778e+08
1/40	-	4.5128e+11	-	20.9644	1.2100e+09	-	20.9826	1.2100e+09
	L Scheme		L Scheme			L Scheme		
				cond. #			cond. #	
dx	# iterations	condition #	# iterations	Richards	Transport	# iterations	Richards	Transport
1/10	10000	1.1768e+04	4000	5.000	6.2544e+03	3000	5.000	6.2544e+03
1/20	26000	2.5237e+04	16000	5.000	1.4067e+04	6000	5.000	1.4067e+04
1/40	-	5.1895e+04	44000	5.000	2.8441e+04	12000	5.000	2.8440e+04
	Picard		Picard			Picard		
				cond. #			cond. #	
dx	# iterations	condition #	# iterations	Richards	Transport	# iterations	Richards	Transport
1/10	-	4.4870e+10	-	20.9641	3.2267e+08	-	20.9726	3.2267e+08
1/20	-	2.4617e+11	-	20.9642	5.3778e+08	-	20.9732	5.3778e+08
1/40	-	9.0255e+11	-	20.9644	1.2100e+09	-	20.9752	1.2100e+09

Table 8: Example 2B: variably saturated medium, fixed dt = dx/100

	Monolithic		NonLinS			AltLinS		
	Newton		Newton			Newton		
			cond. #			cond. #		
dt	# iterations	condition #	# iterations	Richards	Transport	# iterations	Richards	Transport
1/1000	-	2.2435e+10	-	20.9641	3.2267e+08	-	20.9795	3.2267e+08
1/2000	-	2.2444e+10	-	20.9641	6.4533e+08	-	20.9799	6.4533e+08
1/4000	-	2.2461e+10	20000	20.9640	1.2907e+09	-	20.9807	1.2907e+09
	L Scheme		L Scheme			L Scheme		
			cond. #			cond. #		
dt	# iterations	condition #	# iterations	Richards	Transport	# iterations	Richards	Transport
1/1000	10000	1.1768e+04	4000	5.000	6.2544e+03	3000	5.000	6.2544e+03
1/2000	14000	5.9591e+03	6000	5.000	3.2036e+03	6000	5.000	3.2036e+03
1/4000	20000	3.0483e+03	12000	5.000	1.6697e+03	12000	5.000	1.6697e+03
	Picard		Picard			Picard		
			cond. #			cond. #		
dt	# iterations	condition #	# iterations	Richards	Transport	# iterations	Richards	Transport
1/1000	-	4.4870e+10	-	20.9641	3.2267e+08	-	20.9726	3.2267e+08
1/2000	-	2.4617e+11	-	20.9642	6.4533e+08	-	20.9731	6.4533e+08
1/4000	-	9.0255e+11	-	20.9644	1.2907e+09	-	20.9739	1.2907e+09

Table 9: Example 2B: variably saturated medium, fixed dx=1/10

5 Conclusions

In this paper we considered surfactant transport in variably saturated porous media. The water flow and the transport are in this case fully coupled. Three linearization techniques were considered: the Newton method, the modified Picard and the *L*-scheme. Based on these, monolithic and splitting schemes were designed, analyzed and numerically tested. We conclude that the only quadratic convergent scheme is the monolithic Newton, that the *L*-scheme based solvers are the most robust ones and produce well-conditioned linear systems and that the alternative schemes are faster than the classical splitting approaches.

Acknowledgements The research of D. Illiano and F.A. Radu was funded by VISTA, a collaboration between the Norwegian Academy of Science and Letters and Equinor. The research of I.S. Pop was supported by the Research Foundation-Flanders (FWO), Belgium through the Odysseus programme (project G0G1316N) and Equinor through the Akademia grant.
We thank our colleagues from the *Sintef* research group. In particular Olav Møyner PhD, for assistance with the implementation of the numerical examples in *MRST*, the toolbox based on Matlab developed at *Sintef* itself.

References

1. I. Aavatsmark, *An introduction to multipoint flux approximations for quadrilateral grids, Computational Geosciences Volume 6, Issue 3-4, Pages 405-432* , 2002.
2. A. Agosti, L. Formaggia, A. Scotti, *Analysis of a model for precipitation and dissolution coupled with a Darcy flux, J. Math. Anal. Appl. 431, Issue 2, Pages 752-781*, 2015.
3. W. Alt, H. Luckhaus, *Quasilinear elliptic-parabolic differential equations, S. Math Z, Volume 183, Issue 3, Pages 311–341* , 1983.
4. T. Arbogast, M. F. Wheeler, *A nonlinear mixed finite element method for a degenerate parabolic equation arising in flow in porous media, SIAM J. Numer. Anal., Volume 33, Issue 4, Pages 1669–1687*, 1996.
5. J. W. Barrett, P. Knabner, *Finite element approximation of the transport of reactive solutes in porous media. Part 1: error estimates for nonequilibrium adsorption processes, SIAM J. Numer. Anal., Volume 34, Issue 1, Pages 201-227*, 1997.
6. M. Bause, J. Hoffmann, P. Knabner, *First-order convergence of multi-point flux approximation on triangular grids and comparison with mixed finite element methods, Numer. Math., Volume 116, Issue 1, Pages 1-29* , 2010.

7. M. Berardi, F. Difonzo, M. Vurro, L. Lopez, *The 1D Richards' equation in two layered soils: a Filippov approach to treat discontinuities, Adv Water Resour, Volume 115, Pages 264-272* , 2018.
8. L. Bergamaschi, M. Putti, *Mixed finite elements and Newton-type linearizations for the solution of Richards' equation, Int. J. Num. Meth. Engng., Volume 45, Issue 8, Pages 1025-1046*, 1999.
9. K. Brenner, C. Cances, *Improving Newton's method performance by parametrization: The case of the Richards equation, SIAM J. Numer. Anal., Volume 55, Pages 1760–1785*, 2017.
10. C. Cances, I.S. Pop, M. Vohralik, *An a posteriori error estimate for vertex-centered finite volume discretizations of immiscible incompressible two-phase flow, Math. Comp. Vol. 83, Pages 153-188*, 2014.
11. M. Celia, E. Bouloutas, R. L. Zarba *A General Mass-Conservative Numerical Solution for the Unsaturated Flow Equation, Adv Water Resour, Volume 26, Issue 7, Pages 1483-1496*, 1990.
12. N. Christofi, I. B. Ivshina, *Microbial surfactants and their use in field studies of soil remediation, J. Appl. Microbiol., Volume 93, Issue 6, Pages 915-929* , 2002.
13. C. Dawson, *Analysis of an upwind-mixed finite element method for nonlinear contaminant transport equations, SIAM J. Numer. Anal., Volume 35, Issue 5, Pages 1709– 1724*, 1998.
14. R. Eymard, M. Gutnic, D. Hilhorst, *The finite volume method for Richards equation, Comput. Geosci., Volume 3, Issue 3-4, Pages 256–294*, 1999.
15. R. Eymard, D. Hilhorst, M. Vohral, *A combined finite volume- nonconforming/mixed-hybrid finite element scheme for degenerate parabolic problems, Numer. Math., Volume 105, Issue 1, Pages 73–131*, 2006.
16. M.W. Farthing, F.L. Ogden, *Numerical Solution of Richards' Equation: A Review of Advances and Challenges, Soil Sci. Soc. Amer. J. Volume 81, Pages 1257–1269*, 2017.
17. C. Gallo, G. Manzini, *A mixed finite element/finite volume approach for solving biodegradation transport in groundwater, Int. J. Numer. Meth. Fl., Volume26, Issue 5, Pages 533-556*, 1998.
18. M. van Genuchten, *A Closed-form Equation for Predicting the Hydraulic Conductivity of Unsaturated Soils, Soil Sci. Soc. Am. J. 44(5)*, 1980.
19. R. Helmig, *Multiphase flow and transport processes in the subsurface: a contribution to the modeling of hydrosystems, Springer-Verlag* , 1997.
20. E. J. Henry, J. E. Smith, A. W. Warrick, *Solubility effects on surfactant-induced unsaturated flow through porous media, Journal of Hydrology, Volume 223, Issues 3–4*, 1999.
21. D Husseini, *Effects of Anions acids on Surface Tension of Water, Undergraduate Research at JMU Scholarly Commons*, 2015.
22. W. Jäger, J. Kačur, *Solution of porous medium type systems by linear approximation schemes, Numer. Math., Volume 60, Pages 407–427*, 1991.
23. A. Karagunduz, M. H. Young, K. D. Pennell, *Influence of surfactants on unsaturated water flow and solute transport, Water Resour. Res., Volume 51, Issue 4, Pages 1977-1988*, 2015.
24. R. A. Klausen, F. A. Radu, G. T. Eigestad, *Convergence of MPFA on triangulations and for Richards' equation, Int. J. Numer. Meth. Fl., Volume 58, Issue 12, Pages 1327-1351*, 2008.
25. R Klausen, FA Radu, P Knabner, *Optimal order convergence of a modified BDM1 mixed finite element scheme for reactive transport in porous media, Int. J. Numer. Meth. Fluids Volume 58, Pages 1327–1351*, 2008.
26. P. Knabner, S. Bitterlich, R. I. Teran, A. Prechtel, E. Schneid, *Influence of Surfactants on Spreading of Contaminants and Soil Remediation, Springer*, 2003.
27. K. Kumar, I. S. Pop, F. A. Radu, *Convergence analysis of mixed numerical schemes for reactive flow in a porous medium, SIAM J. Numer. Anal., Volume 51, Issue 4, Pages 2283-2308*, 2013.
28. K.-A. Lie, *An Introduction to Reservoir Simulation Using MATLAB: User guide for the Matlab Reservoir Simulation Toolbox (MRST), SINTEF ICT*, 2016
29. F. List, F. A. Radu, *A study on iterative methods for solving Richards' equation, Comput. Geosci., Volume 20, Issue 2, Pages 341–353*, 2016.
30. K Mitra, IS Pop, *A modified L-Scheme to solve nonlinear diffusion problems, Comput. Math. Appl. Volume 77, Pages 1722-1738* 2019.
31. R. Nochetto, C. Verdi, *Approximation of degenerate parabolic problems using numerical integration. SIAM J. Numer. Anal. 25, Pges 784–814*, 1988.
32. A. Prechtel, P. Knabner, *Accurate and efficient simulation of coupled water flow and nonlinear reactive transport in the saturated and vadose zone - application to surfactant enhanced and intrinsic bioremediation, Int. J. Water Resour. D.,Volume 47, Pages 687-694*, 2002.
33. I. S. Pop, F. A. Radu, P. Knabner, *Mixed finite elements for the Richards' equation: linearization procedure, J. Comput. Appl. Math., Volume 168, Issue 1, Pages 365-373*, 2004.

34. F. A. Radu, I. S. Pop, S. Attinger, *Analysis of an Euler implicit, mixed finite element scheme for reactive solute transport in porous media, Numer. Methods Partial. Differ. Equ., Volume 26, Issue 2, Pages 320-344* 2010.
35. F. A. Radu, I. S. Pop, P. Knabner, *Order of convergence estimates for an Euler implicit, mixed finite element discretization of Richards' equation, SIAM J. Numer. Anal., Volume 42, Issue 4, Pages 1452-1478*, 2004.
36. FA Radu, IS Pop, P Knabner, *On the convergence of the Newton method for the mixed finite element discretization of a class of degenerate parabolic equation, Numerical Mathematics and Advanced Applications, A. Bermudez de Castro, D. Gomez, P. Quintela, P. Salgado (Eds.), Springer-Verlag Heidelberg, Pages 1192-1200*, 2006.
37. F. A. Radu, N. Suciu, J. Hoffmann, A. Vogel, O. Kolditz, C. H. Park, S. Attinger, *Accuracy of numerical simulations of contaminant transport in heterogeneous aquifers: a comparative study, Adv. Water Resour., Volume 34, Issue 1, Pages 47–61*, 2011.
38. T. F. Russell, M. F. Wheeler, *Finite element and finite difference methods for continuous flows in porous media, SIAM, 35-106.*, 1983.
39. M. Slodicka, *A robust and efficient linearization scheme for doubly non-linear and degenerate parabolic problems arising in flow in porous media, SIAM J. Sci. Comput., Volume 23, Issue 5, Pages 1593–1614.*, 2002.
40. J. E. Smith, R. W. Gillham, *The effect of concentration-dependent surface tension on the flow of water and transport of dissolved organic compounds: A pressure head-based formulation and numerical model, Water Resour. Res., Volume 31, Issue 3, Pages 795*, 1994.
41. J Smith, R Gillham, *Effects of solute concentration-dependent surface tension on unsaturated flow: Laboratory sand column experiments, Water Resource Research Volume 35, Issue 4, Pages 973–982*, 1999.
42. N. Suciu, *Diffusion in random velocity fields with applications to contaminant transport in groundwater, Water Resour. Res., Volume 69, Pages 114-133*, 2014.
43. M. Vohralik, *A posteriori error estimates for lowest-order mixed finite element discretizations of convection-diffusion-reaction equations, SIAM J. Numer. Anal. Volume Volume 45, Issue 4, Pages 1570-1599*, 2007.
44. C. S. Woodward, C. N. Dawson, *Analysis of expanded mixed finite element methods for a nonlinear parabolic equation modeling flow into variably saturated porous media, SIAM J. Numer. Anal. Volume 37, Issue 3, Pages 701-724*, 2000.
45. WA Yong, IS Pop, *A numerical approach to porous medium equations, Preprint 95-50 (SFB 359), IWR. University of Heidelberg*, 1996.

UHasselt Computational Mathematics Preprint Series

2019

UP-19-05 *D. Illiano, I.S. Pop, F.A. Radu*, **Iterative schemes for surfactant transport in porous media**, 2019

UP-19-04 *M. Bastidas, C. Bringedal, I.S. Pop, F.A. Radu*, **Adaptive numerical homogenization of nonlinear diffusion problems**, 2019

UP-19-03 *K. Kumar, F. List, I.S. Pop, F.A. Radu*, **Formal upscaling and numerical validation of fractured flow models for Richards' equation**, 2019

UP-19-02 *M.A. Endo Kokubun, A. Muntean, F.A. Radu, K. Kumar, I.S. Pop, E. Keilegavlen, K. Spildo*, **A pore-scale study of transport of inertial particles by water in porous media**, 2019

UP-19-01 *Carina Bringedal, Lars von Wolff, and Iuliu Sorin Pop*, **Phase field modeling of precipitation and dissolution processes in porous media: Upscaling and numerical experiments**, 2019

2018

UP-18-09 *David Landa-Marbán, Gunhild Bodtker, Kundan Kumar, Iuliu Sorin Pop, Florin Adrian Radu*, **An upscaled model for permeable biofilm in a thin channel and tube**, 2018

UP-18-08 *Vo Anh Khoa, Le Thi Phuong Ngoc, Nguyen Thanh Long*, **Existence, blow-up and exponential decay of solutions for a porous-elastic system with damping and source terms**, 2018

UP-18-07 *Vo Anh Khoa, Tran The Hung, Daniel Lesnic*, **Uniqueness result for an age-dependent reaction-diffusion problem**, 2018

UP-18-06 *Koondanibha Mitra, Iuliu Sorin Pop*, **A modified L-Scheme to solve nonlinear diffusion problems**, 2018

UP-18-05 *David Landa-Marban, Na Liu, Iuliu Sorin Pop, Kundan Kumar, Per Pettersson, Gunhild Bodtker, Tormod Skauge, Florin A. Radu*, **A pore-scale model for permeable biofilm: numerical simulations and laboratory experiments**, 2018

UP-18-04 *Florian List, Kundan Kumar, Iuliu Sorin Pop and Florin A. Radu*, **Rigorous upscaling of unsaturated flow in fractured porous media**, 2018

UP-18-03 *Koondanibha Mitra, Hans van Duijn*, **Wetting fronts in unsaturated porous media: the combined case of hysteresis and dynamic capillary**, 2018

UP-18-02 *Xiulei Cao, Koondanibha Mitra*, **Error estimates for a mixed finite element discretization of a two-phase porous media flow model with dynamic capillarity**, 2018

UP-18-01 *Klaus Kaiser, Jonas Zeifang, Jochen Schütz, Andrea Beck and Claus-Dieter Munz*, **Comparison of different splitting techniques for the isentropic Euler equations**, 2018

2017

UP-17-12 *Carina Bringedal, Tor Eldevik, Øystein Skagseth and Michael A. Spall*, **Structure and forcing of observed exchanges across the Greenland-Scotland Ridge**, 2017

UP-17-11 *Jakub Wiktor Both, Kundan Kumar, Jan Martin Nordbotten, Iuliu Sorin Pop and Florin Adrian Radu*, **Linear iterative schemes for doubly degenerate parabolic equations**, 2017

UP-17-10 *Carina Bringedal and Kundan Kumar*, **Effective behavior near clogging in upscaled equations for non-isothermal reactive porous media flow**, 2017

UP-17-09 *Alexander Jaust, Balthasar Reuter, Vadym Aizinger, Jochen Schütz and Peter Knabner*, **FESTUNG: A MATLAB / GNU Octave toolbox for the discontinuous Galerkin method. Part III: Hybridized discontinuous Galerkin (HDG) formulation**, 2017

UP-17-08 *David Seus, Koondanibha Mitra, Iuliu Sorin Pop, Florin Adrian Radu and Christian Rohde*, **A linear domain decomposition method for partially saturated flow in porous media**, 2017

UP-17-07 *Klaus Kaiser and Jochen Schütz*, **Asymptotic Error Analysis of an IMEX Runge-Kutta method**, 2017

UP-17-06 *Hans van Duijn, Koondanibha Mitra and Iuliu Sorin Pop*, **Travelling wave solutions for the Richards equation incorporating non-equilibrium effects in the capillarity pressure**, 2017

UP-17-05 *Hans van Duijn and Koondanibha Mitra*, **Hysteresis and Horizontal Redistribution in Porous Media**, 2017

UP-17-04 *Jonas Zeifang, Klaus Kaiser, Andrea Beck, Jochen Schütz and Claus-Dieter Munz*, **Efficient high-order discontinuous Galerkin computations of low Mach number flows**, 2017

UP-17-03 *Maikel Bosschaert, Sebastiaan Janssens and Yuri Kuznetsov*, **Switching to nonhyperbolic cycles from codim-2 bifurcations of equilibria in DDEs**, 2017

UP-17-02 *Jochen Schütz, David C. Seal and Alexander Jaust*, **Implicit multiderivative collocation solvers for linear partial differential equations with discontinuous Galerkin spatial discretizations**, 2017

UP-17-01 *Alexander Jaust and Jochen Schütz*, **General linear methods for time-dependent PDEs**, 2017

2016

UP-16-06 *Klaus Kaiser and Jochen Schütz*, **A high-order method for weakly compressible flows**, 2016

UP-16-05 *Stefan Karpinski, Iuliu Sorin Pop, Florin A. Radu*, **A hierarchical scale separation approach for the hybridized discontinuous Galerkin method**, 2016

UP-16-04 *Florin A. Radu, Kundan Kumar, Jan Martin Nordbotten, Iuliu Sorin Pop*, **Analysis of a linearization scheme for an interior penalty discontinuous Galerkin method for two phase flow in porous media with dynamic capillarity effects** , 2016

UP-16-03 *Sergey Alyaev, Eirik Keilegavlen, Jan Martin Nordbotten, Iuliu Sorin Pop*, **Fractal structures in freezing brine**, 2016

UP-16-02 *Klaus Kaiser, Jochen Schütz, Ruth Schöbel and Sebastian Noelle*, **A new stable splitting for the isentropic Euler equations**, 2016

UP-16-01 *Jochen Schütz and Vadym Aizinger*, **A hierarchical scale separation approach for the hybridized discontinuous Galerkin method**, 2016